Neutron scattering study of the picosecond dynamics of polybutadiene and polyisoprene

R. Zorn,[1] A. Arbe,[1] J. Colmenero,[2] B. Frick,[3] D. Richter,[1] and U. Buchenau[1]

[1]*Institut für Festkörperforschung, Forschungszentrum Jülich, G-52425 Jülich, Germany*

[2]*Departamento de Fisica de Materiales, Universidad del Pais Vasco, Apartado 1072, E-20080 San Sebastian, Spain*

[3]*Institut Laue-Langevin, Boîte Postale 156, F-38042 Grenoble Cédex 6, France*

Neutron time-of-flight data of polybutadiene and polyisoprene in a wide temperature range around the glass transition are reported. The anharmonic part of the spectra is evaluated using a recently developed time domain Fourier transform technique. The results corroborate the recent finding of two different time domains in the dynamics, one above a crossover time of about 2 ps and the other below it. Two different interpretations of the short time behavior are considered, namely a fast Debye regime of the α relaxation and a vibrational softening of the boson peak.

PACS number(s): 64.70.Pf, 61.12.−q, 61.41.+e

I. INTRODUCTION

The dynamics of polymers and other glass formers at the glass transition is still a puzzle. One of the open questions is the nature of the so-called "fast process" observed in the picosecond range by neutron and light scattering [1–3]. These experiments reveal strong seemingly quasielastic intensities appearing in the spectra first somewhat below T_g. With increasing temperature this extra scattering increases strongly, thereby keeping constant the "quasielastic linewidth" which corresponds to processes in the picosecond regime. Compared to the boson peak [4] which is in general observed at low temperatures the characteristic width of the higher temperature quasielastic lines is of similar magnitude. Because of its apparently quasielastic nature, this extra scattering has been interpreted in terms of a fast relaxation process, which was also associated with the β relaxation of the mode coupling theory [5–8]. However, because of its unusual temperature dependence there have always also been suspicions that this fast process is of vibrational origin [9]. These observations which relate to the ω regime find their counterpart in Fourier transformed spectra exhibiting a fast initial decay, which is then followed by a relaxation process of clearly different qualitative features.

Recently, these two aspects, namely, the interpretation of the fast process as an elementary relaxational step [10] in the spirit of Ngai's coupling scheme [11] or its description by vibrational softening and associated relaxation processes in an anharmonic potential in terms of the vibration relaxation model [12], have each been considered by some of us. In the following we describe both approaches briefly.

The first point of view was taken in a recent analysis [10] of time-of-flight (TOF) neutron scattering data studying the picosecond dynamics of polyvinylchloride (PVC). The incoherent intermediate scattering function $S(Q,t)$ corresponding to the nonharmonic additional scattering appearing around T_g was obtained by a procedure which involves deconvolution by harmonic spectra and Fourier transform to the time domain. The time dependence of the thus obtained $S(Q,t)$ shows two different dynamical regimes separated by a crossover time $t_c \approx 2$ ps, which hardly depends on T and Q, at least within the experimental uncertainties. At $t < t_c$ the normalized $S(Q,t)$ could be well described by a simple exponential decay with a relaxation time which depends on Q and T as $\tau_D(Q,T) \propto Q^{-2}\exp[E/RT]$. The activation energy found, $E \approx 5$ kcal/mol, is in the range one can expect for the rotational isomerism barrier in PVC [13,14]. At $t > t_c$ and high temperature $(T \approx T_g + 100$ K) the $S(Q,t)$ behavior is consistent with the Kohlrausch-Williams-Watts (KWW) $S(Q,t) = \exp[-(t/\tau_{KWW})^\beta]$ deduced from backscattering neutron data in the time range $10^{-10} < t < 10^{-8}$ s. The β value $(\beta \approx 0.23)$ is similar and also the Q and T dependence of τ_{KWW}. It is interesting to point out that these results are in principle in good agreement [15] with the assumptions of the coupling scheme which was proposed a long time ago by Ngai [11]. This approach assumes that below a characteristic time t_c a given relaxing unit behaves as if uncoupled from the system (Debye-like "primitive motion"). At higher times, the effects of correlations set in and the dynamics is modified towards a KWW behavior. The order of magnitude of t_c is not given in the model but it is supposed to be shorter than 10^{-10} s. From the behavior of $S(Q,t)$ in PVC described above, it is also possible to deduce [15] an empirical relationship between $\tau_D(Q,T)$ and $\tau_{KWW}(Q,T)$, which turns out to be similar to the so-called "second universality" of the coupling scheme.

However, PVC is an unusual polymer due to both the very low value of the KWW shape parameter $(\beta \approx 0.2)$ and the extremely fragile [16] character $(D \approx 3)$. According to the recently proposed [17] empirical relationship between fragility and the intensity of the low frequency excitations (boson peak) the incoherent TOF spectra of PVC do not show any clear evidence of a boson peak even at temperatures below T_g. Moreover, the boson peak has not been observed up to date in the low frequency Raman spectra of PVC [18]. Therefore, one important question now is to know if the results obtained in PVC are a general feature of glass-forming polymers or in con-

trast are consequences of the particular character of PVC.

The other approach was recently taken in order to interpret neutron data on the fast process in polycarbonates [12]. There, the softening of the boson peak and onset of relaxations below the glass transition were explained in terms of the vibration relaxation model which postulates a vibrational origin of the fast process. At the basis of this assumption are three experimental observations. (i) In many glass-forming systems at larger energy transfers ($\hbar\omega \geq 2$ meV) the scattering function in the region where Bose scaling holds exhibits a $1/\omega$ tail indicating a density of states $g(\omega) \sim \omega$ [19]. (ii) At low frequencies from Brillouin light scattering strongly temperature dependent sound velocities are found near the glass transition [20] (variations are typically on the order of a factor of 2) implying a strong increase of the sound wave density of states (correspondingly by about a factor of 8) and consequently of the low frequency vibrational scattering. (iii) Furthermore, vibrational softening of the boson peak has been found in several substances [3,12,19,21].

Dwelling on these observations, the vibration relaxation model starts by ascribing the proportionality of $g(\omega)$ to ω to the spectrum of a random dynamical matrix [22], which in addition has the feature of an equal density of positive and negative eigenvalues around $\hbar\omega \approx 0$. Anharmonic potentials due to negative eigenvalues have a double minimum shape which naturally implies fast local hopping processes over the potential barrier. In the Kramers weak coupling approximation [23] these hopping processes are associated with the phonon damping and are considered to be the fastest relaxation processes in the glass or undercooled liquid. The scattering function combining the slow damped vibrations and the associated relaxations is calculated in Gaussian approximation using a Langevin approach.

In this concept, which was very successful in the interpretation of the polycarbonate spectra, the Q^2 dependence of the fast process is a natural consequence of phonon scattering and t_c is the crossover time between vibrations and relaxations.

In this paper, trying to address the question of the nature of the fast process, we have analyzed TOF data corresponding to other polymers, polybutadiene (PB) and polyisoprene (PI-d3), by following the same procedure as in the case of PVC [10]. Moreover, we have also evaluated TOF data corresponding to a fully deuterated PB, i.e., coherent scattering. The results obtained are discussed in the framework of the above-mentioned approaches. A critical revision of the deconvolution procedure used for analyzing the data as well as the approximations involved is also included in Sec. III.

II. EXPERIMENT

A. Sample preparation

All samples used in this investigation were linear polydienes synthesized by anionic polymerization [24]. This technique yields small polydispersities $M_w/M_n < 1.1$. By choosing the conditions of the synthesis the microstruc-

ture of the product can be controlled. For all samples this has been done in a way to minimize the number of unwanted side groups (vinyl in the case of PB, 3,4 in the case of PI) so that for the PB's essentially backbone polymers were obtained and the side groups of PI were mainly methyl groups. Due to the irregular sequence of bond orientation (*trans, gauche*) crystallization is inhibited and a glassy state is obtained even at the smallest cooling rates.

Protonated polybutadiene (PB) was synthesized with a molecular weight $M_w = 8 \times 10^4$ and a microstructure of 47% *cis*, 46% *trans*, and 7% vinyl monomeric units. The glass transition temperature was $T_g = 186$ K determined by differential scanning calorimetry (DSC). The fully deuterated polybutadiene (PB-d6) had the same microstructure and the molecular weight $M_w = 9.5 \times 10^4$. The polydispersity was determined to be $M_w/M_n = 1.03$ in this case and the glass transition temperature $T_g = 181$ K from a DSC measurement. In polyisoprene (PB-d3) the methyl group was selectively deuterated in order to suppress incoherent scattering from its rapid motion. Here, the molecular weight was $M_w = 7 \times 10^4$ and the content of 3,4 monomeric units was 7% (the *cis:trans* ratio was not determined but can be expected from the conditions of synthesis to be 4:1). Literature values for T_g of similar polyisoprene samples range from 205 [25] to 213 K [26].

B. Neutron scattering experiments

The aim of the inelastic neutron scattering experiment is the determination of the dynamic structure factor (or scattering function) $S(Q,\omega)$ which represents the material specific part of the cross section of scattering a neutron with a certain momentum transfer $\hbar Q$ and energy transfer $\hbar\omega$. It can be decomposed into an incoherent and a coherent contribution, $S_{inc}(Q,\omega)$ and $S_{coh}(Q,\omega)$, respectively. The former is determined by the self-correlation function of the nuclei, the latter by the two-particle correlation function—both Fourier transformed in space and time. Because the self-correlation function does not contain information about the arrangement of nuclei in space, $S_{inc}(Q,\omega)$ does not include any structural information in its Q dependence; its Q dependence is only determined by the spatial extent of the single-particle motion. In contrast, $S_{coh}(Q,\omega)$ usually reflects the spatial order as the static structure factor $S(Q)$ from a diffraction experiment does.

The intensities of both kinds of scattering depend strongly on the nuclei observed. Especially, protons cause an exceptionally strong incoherent scattering ($\sigma_{inc} = 79.7$ b/nucleus, $\sigma_{coh} = 1.8$ b/nucleus) while deuterons give rise to more coherent scattering ($\sigma_{inc} = 2.0$ b/nucleus, $\sigma_{coh} = 5.6$ b/nucleus). This fact can be used to selectively emphasize one or the other by isotopic substitution. In our case (Table I) PB is a nearly completely incoherent scatterer (94% of the total scattering) while PB-d6 is a predominantly coherent scatterer (82% of the total). It has to be noted that the incoherent scattering in the case of PB is to more than 99.98% due to the protons, so that only their dynamic properties determine

NEUTRON SCATTERING STUDY OF THE PICOSECOND . . .

TABLE I. Scattering cross-sections (in b per monomeric unit) for the different samples investigated. The value in parentheses for PI-$d3$ is the contribution of backbone-bound hydrogen nuclei to the incoherent scattering.

Sample	Monomeric unit	σ_{coh}	σ_{inc}	σ_{tot}
PB	$CH_2CH = CHCH_2$	32.8	478.2	511.0
PB-$d6$	$CH_2CD = CDCD_2$	55.8	12.0	67.8
PI-$d3$	$CH_2CH = C(CD_3)CH_2$	53.4	404.5 (398.5)	457.9

$S(Q,\omega)$. For PB-$d6$ the coherent scattering is a mixture of C-C, C-D, and D-D correlation contributions. The scattering of PI-$d3$ is mainly incoherent (88% of the total) and the selective deuteration of the methyl group has the additional effect that it essentially originates from the backbone-bound hydrogen nuclei (98.5% of the incoherent scattering).

The experiments have been performed on the instrument IN6 at the Institut Laue Langevin (ILL). This instrument determines the energy transfer by means of a time-of-flight measurement. Because of its time-focusing technique it provides good scattering intensities. In general about two hours registration time at one temperature were sufficient to obtain reasonable statistics.

The instrument was used with an incident neutron wavelength $\lambda_i = 5.1$ Å yielding an energy resolution of ≈ 90 μeV [full width at half maximum (FWHM)]. The angular range of the detectors of IN6 is $10° < 2\theta < 115°$ which corresponds to a Q range of 0.2–2.1 Å^{-1} for elastic scattering. It has to be noted that the actual Q value for one detector deviates strongly from its "elastic" value for the energy transfers which are of interest here (from -2 to $+10$ meV energy *gain* of the neutron). Thus, a constant-Q interpolation was indispensable and for small Q values the range of energy transfers obtained was strongly restricted.

PB-$d6$ and PI-$d3$ were measured in flat sample containers put at an angle of 135° with respect to the incident beam in order to avoid self-shielding and self-absorption effects. The same was done for PB by using a hollow cylinder. Residual self-shielding and self-absorption effects were corrected by the CROSSX computer routine developed at the ILL. Multiple scattering was reduced by preparing thin samples with low scattering probabilities (measured transmissions: PB 93%, PB-$d6$ 89%, PI-$d3$ 87%).

For the PB and PB-$d6$ samples an "orange" cryostat was used for temperature control which allows a range of 1.5–310 K. In this case the measurement at the lowest achievable temperature was used as the resolution function of the instrument. For PI-$d3$ the ILL "loop" device was applied, which uses liquid nitrogen and cannot achieve temperatures < 80 K. Here, the resolution function was determined by a measurement of an equally shaped vanadium sample.

Figure 1 shows representative TOF spectra from PI-$d3$ (analogous figures for PB and PB-$d6$ can be found in earlier publications [27,28]). The actual data have been in-
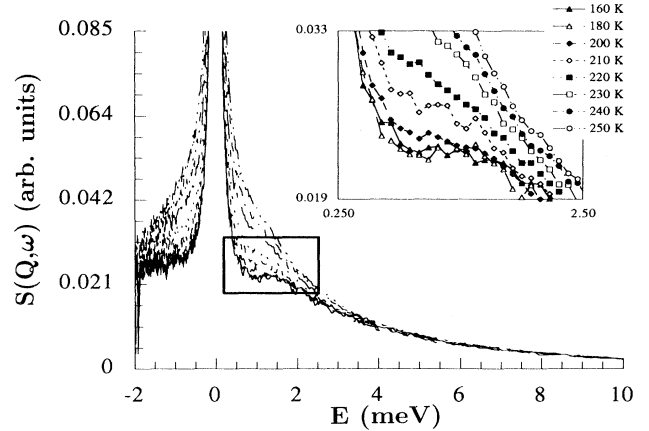

FIG. 1. $S(Q,\omega)$ for PI-$d3$ at different temperatures and scaled with Bose and Debye-Waller factors. The height of the vertical axis (0.085 a.u.) corresponds to 1% of the elastic line maximum. Reference temperature $T = 200$ K. Inset: Magnification showing the additional nonharmonic contribution to the scattering at $T > 180$ K.

terpolated to constant $Q = 1.4$ Å^{-1} and scaled by Bose and Debye-Waller factors. For the temperatures and the energy range shown here this scaling is essentially only a multiplication by a constant factor so that the shape of $S(Q,\omega)$ remains unaffected. For the lowest temperatures at about 1.2 meV the boson peak is faintly visible (see inset)—a feature which is a well known characteristic of spectra from glass-forming materials in neutron and Raman scattering. In this kind of scaling representation the spectra essentially do not change any more below a certain temperature T_f; $T_f \approx 180$ K (PB, PB-$d6$: $T_f \approx 110$ K) [29]. For higher temperatures more and more quasielastic scattering appears, finally covering up the boson peak.

III. DATA ANALYSIS PROCEDURE

The procedure followed in Ref. [10] for analyzing PVC TOF data was based on the following features. It is well known that in the low temperature range below T_g the TOF spectra in the quasielastic range of fragile glass-forming systems only show harmonic or quasiharmonic contributions, i.e., the spectra fall on a master curve when they are properly scaled by Bose and Debye-Waller factors [28]. As the temperature increases towards T_g, nonharmonic additional scattering starts to accumulate mainly at the low energy range below ≈ 3 meV. This contribution, which grows in intensity as the temperature is increased through T_g, arises from the so-called fast dynamics mentioned in the Introduction. The temperature range at which this additional scattering emerges is usually located in the range $T_g - 50$ K, i.e., in the range of the Vogel temperature T_0, where the Vogel-Fulcher expression for the temperature dependence of the viscosity diverges. However, it has recently been reported [12] that in the case of two different polycarbonates this T range is located well below T_g.

The nonharmonic contribution to the spectra can be obtained by means of a deconvolution procedure in the

framework of the following approximations. (i) The harmonic behavior of vibrations observed at $T < T_g$ is extrapolated to high temperature, i.e., a temperature independent vibrational density of states is assumed. (ii) The harmonic and the nonharmonic components of the spectra are considered as statistically independent processes. Some questions associated with these two approximations will be discussed in Sec. V B.

In this framework, we can write a model scattering function as a convolution product

$$S(Q,\omega) \equiv S^{\text{rela}}(Q,\omega) \otimes S^{\text{harm}}(Q,\omega) , \tag{1}$$

where we have adopted the term "rela" (relaxation) for the nonharmonic scattering. To compare this model function to the experimental curves we have to convolute the expression in Eq. (1) with the measured instrumental resolution function $R(Q,\omega)$. Therefore the experimental spectra should be given in this framework by

$$S^{\text{expt}}(Q,\omega) = S^{\text{rela}}(Q,\omega) \otimes S^{\text{harm}}(Q,\omega) \otimes R(Q,\omega) . \tag{2}$$

We can rewrite Eq. (2) as

$$S(Q,\omega) = S^{\text{rela}}(Q,\omega) \otimes R^{\text{effect}}(Q,\omega) , \tag{3}$$

where $R^{\text{effect}}(Q,\omega)$ plays the role of an effective resolution for the so-called relaxation process given by

$$R^{\text{effect}}(Q,\omega) = S^{\text{harm}}(Q,\omega) \otimes R(Q,\omega) .$$

Therefore $R^{\text{effect}}(Q,\omega)$ is the experimental scattering curve corresponding to harmonic vibrations at the temperature considered. It can be obtained from the harmonic spectra at low temperature $(T \lesssim T_f)$ properly scaled by the Bose and Debye-Waller factors. Fourier transforming Eq. (3) into the time domain,

$$S^{\text{expt}}(Q,t) = S^{\text{rela}}(Q,t) S^{\text{effect}}(Q,t) . \tag{4}$$

In the following, in order to simplify our notation we will call $S^{\text{rela}}(Q,t) \ S(Q,t)$.

Then we calculate $S(Q,t)$ by dividing the Fourier transformation of the experimental spectra by the Fourier transformation of the effective resolution spectra obtained as described above. The limits of applicability of this deconvolution procedure, as well as the uncertainties of the results obtained, were studied by using several theoretical model functions for $S(Q,\omega)$, mainly Lorentzian functions and Havriliak-Negami functions, which can be considered as good analytical approximations to the numerical Fourier transformation of the KWW intermediate scattering functions [30].

Another interesting point is to compare the above-described deconvolution procedure to another more conventional one, i.e., deconvolution by only the instrumental resolution function. In the harmonic approximation, the intermediate scattering function corresponding to $S^{\text{harm}}(Q,\omega)$ in Eq. (2) should decay in a relatively short time (we will call it t_{ph}) to a constant value, the Debye-Waller factor. This can be seen in Fig. 2 where we have represented the intermediate scattering function for the harmonic part in the case of PB, calculated by deconvolution of the effective resolution at 280 K with the instrumental resolution. In this case t_{ph} can be estimated to be
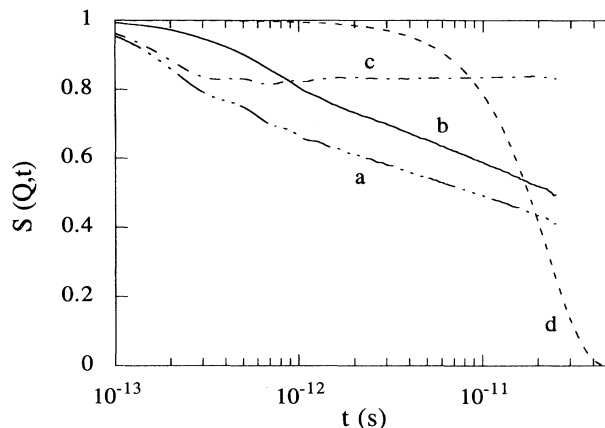

FIG. 2. Comparison between $S(Q,t)$ for $Q = 1.4 \ \text{Å}^{-1}$ calculated from $S(Q,\omega)$ of PB at 280 K by deconvolution of (curve a) the instrumental resolution; (curve b) the effective resolution (see text). $S(Q,t)$ corresponding to the calculated harmonic spectrum (see text) at 280 K is also shown (curve c). Curve d shows the Fourier transformation of the instrumental resolution function.

about 4×10^{-13} s. Therefore, in the framework of approximations (i) and (ii), $S(Q,t)$ and the intermediate scattering function obtained by deconvolution with only the instrumental function should be different only in a constant factor in the time range $t > t_{\text{ph}}$. However, concerning the short time regime where the scattering function is Debye-like, the phonon induced initial reduction is important because t_{ph} is centered in the middle of the Debye regime. Thus deconvolution of the harmonic phonons is important.

In order to avoid cutoff effects from the neutron energy loss side of the spectra, the energy loss side of $S(Q,\omega)$ was calculated from the energy gain side using the detailed balance condition.

IV. RESULTS

Following the general trends of glass-forming polymers described in the preceding sections, the spectra of the three polymers investigated show quasiharmonic behavior until a temperature which depends on the polymer (≈ 120 K for PB and PB-$d6$ and ≈ 180 K for PI-$d3$). Until this temperature the spectra corresponding to each polymer fall onto a master curve when they are properly Bose and Debye Waller factor scaled (see Fig. 1 as an example). At higher temperatures, a nonharmonic additional component arises in the scattering at low energies ($E < 3$ meV) and increases with temperature beyond the harmonic expectation (see Fig. 1).

In order to obtain $S(Q,t)$ we have applied to these results the analyzing procedure described in the preceding section. In the cases of both PB and PB-$d6$ we have chosen the quasiharmonic spectra at 100 K for constructing the effective resolution. In the case of PI-$d3$ we have used the spectra at 180 K.

Figure 3 shows the normalized intermediate scattering

function $S(Q,t)$ for the three polymers investigated and for different temperatures and Q values. In the cases of PB and PI-$d3$, as the scattering is dominated by the incoherent contribution, $S(Q,t)$ corresponds to the self-correlation function of protons. However, in the case of PB-$d6$ the scattering is mainly coherent. Therefore
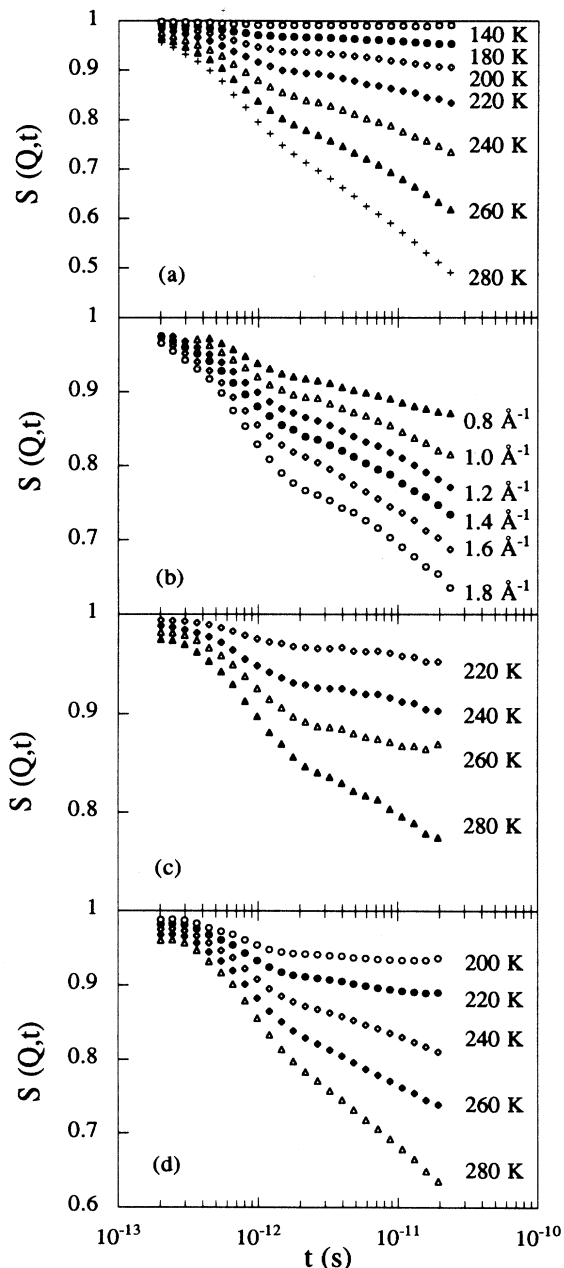
$S(Q,t)$ is a two-particle correlation function. In Fig. 3(d), this function is represented for a value of $Q=1.40$ Å^{-1} which corresponds to the peak of the static structure factor [31]. This implies that $S(Q,t)$ reflects in this case mainly the interchain correlations. The time behavior of $S(Q,t)$ shown in Fig. 3 is the same as the reported one for PVC [10], i.e., a two-step decay separated by a crossover time $t_c \approx 1-2$ ps, which hardly depends on both Q and temperature.

In the cases of PB and PI-$d3$ (incoherent scattering) we can calculate a mean squared displacement of the scattering centers $\langle r^2(t) \rangle$ from the $S(Q,t)$ obtained as

$$\langle r^2(t) \rangle = (6/Q^2)\ln[1/S(Q,t)] \; .$$

If the Gaussian approximation is verified the behavior obtained for $\langle r^2(t) \rangle$ at a given temperature should be Q independent. This was the behavior obtained for PVC [10]. However, in the cases of PB and PI-$d3$, although the calculated time dependence of $\langle r^2(t) \rangle$ of each polymer is similar for all the Q values investigated, the absolute values are different, indicating deviations from the Gaussian approximation. The behavior found indicates that $S(Q,t)$ can be written as

$$S(Q,t) = \exp[-Q^b f(t)/6] \; , \tag{5}$$

where $b < 2$. Here $f(t)$, giving the time dependence of the intermediate scattering function, is no longer an actual mean squared displacement. However, $f(t)$ calculated as $f(t) = (6/Q^b)\ln[1/S(Q,t)]$ should not depend on Q. Figure 4 shows that this is true, within the experimental uncertainty, for $b = 1.4$ in the case of PB and $b = 1.3$ in the case of PI-$d3$. $f(t)$ shows two dynamical regimes separated by the crossover time defined above. $f(t)$ can be expressed as
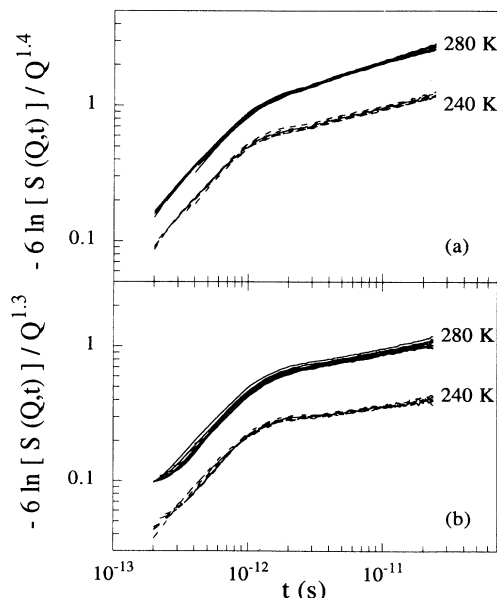

FIG. 3. Normalized intermediate incoherent scattering function $S(Q,t)$. (a) PB: temperature dependence for $Q = 1.4$ Å^{-1}; (b) PB: Q dependence at $T = 240$ K; (c) PI-$d3$: temperature dependence for $Q = 1.4$ Å^{-1}; (d) PB-$d6$: temperature dependence for the Q value ($Q = 1.4$ Å^{-1}) corresponding to the maximum of the static structure factor (coherent scattering function).

FIG. 4. Time dependence of $S(Q,t)$: (a) PB; (b) PI-$d3$. Different lines at each temperature correspond to different Q values.

$$f(t) \propto \begin{cases} t, & t < t_c \\ t^{\beta}, & t > t_c , \end{cases} \tag{6}$$

where the β value depends on the polymer and on the temperature for each polymer. In the high temperature range ($T \approx T_g + 100$ K), the value of β found is $\beta = 0.3$ for PB and $\beta = 0.2$ for PI-$d3$. As the temperature decreases towards T_g, the value of β also decreases for both polymers. Therefore, apart from the question of the Gaussianity of $S(Q,t)$, the results that were obtained for PVC are now confirmed for other polymers, i.e., they are not associated with the particular character of PVC.

It is interesting to point out that the expression obtained for $S(Q,t)$ in the time range $t > t_c$ corresponds to a KWW function given by $S(Q,t) = \exp[-Q^{b/\beta}C(T)t^{\beta}]$ where $C(T)$ is a temperature coefficient. This expression can be rewritten as $S(Q,t) = \exp\{-[t/\tau(Q,T)]^{\beta}\}$ where the Q dependence of $\tau(Q,T)$ is given by $\tau(Q,T) \propto Q^{-n}$ with $n = b/\beta$. In the high temperature range of PB, the results obtained imply $\beta = 0.3$ and $n = 4.7$. A similar functional form for $S(Q,t)$ with similar values of these parameters ($\beta = 0.3$ and $\langle n \rangle = 4.8$) was obtained for the α relaxation of PB from neutron backscattering (IN13, ILL Grenoble) results (see [28]).

Concerning the question of the Gaussian behavior, it is interesting to recall that it has been found that the Gaussian approximation is approximately followed by the intermediate scattering function of the α relaxation (at least in the high temperature range) in several structurally different polymers [32]. The deviations found for PB and PI-$d3$ could be related to the anisotropy introduced in the main chain by the presence of double bonds randomly distributed.

More generally, one could assume that as a consequence of the disorder present in a glass some atoms undergo larger mean square displacements than others, giving rise to an anomalous Debye-Waller factor. Recent multidimensional NMR results on slow relaxations in a molecular glass point in this direction. However, this question is beyond the objectives of this paper and will be the subject of future work.

V. DISCUSSION

As outlined in the Introduction, we shall take two possible views in interpreting the neutron results. The first is phenomenological and interprets both the short and longer time processes in polybutadiene (once the harmonic phonons are removed) as relaxational phenomena, thus following the line of arguments recently taken for PVC. In this concept the initial decay in $S(Q,t)$ is due to a short time Debye process while the long time tail represents the initial part of the KWW function describing the α relaxation. In a second step we develop a model which is based on the interpretation of the fast initial decay of the intermediate scattering function as due to vibrations. On the basis of a simple soft potential model we relate relaxations and vibrations. This vibration relaxation model is then compared with the intermediate scattering functions for polybutadiene and polyisoprene.

A. Phenomenological interpretation

Taking into account the results obtained in the preceding section [expressions (5) and (6)] we can write the normalized intermediate scattering function $S(Q,t)$ as

$$S(Q,t) = \begin{cases} \exp\left\{-\dfrac{t}{\tau_D(Q,T)}\right\}, & t < t_c \\ \exp\left\{-\left[\dfrac{t}{\tau_{KWW}(Q,T)}\right]^{\beta}\right\}, & t > t_c , \end{cases} \tag{7}$$

i.e., a Debye-like behavior in the fast regime ($t < t_c$) and a KWW one in the slow regime ($t > t_c$). In these expressions, the Q dependence of the characteristic times τ_D and τ_{KWW} should be given by $\tau_D \propto Q^{-b}$ and $\tau_{KWW} \propto Q^{-b/\beta}$ according to Eq. (5). Then we have fitted $S(Q,t)$ shown in Fig. 3 to Eq. (7). In the case of the slow regime ($t > t_c$), we have restricted our analysis to the high temperature range ($T = 240$, 260, and 280 K) of PB where the β value found varies slightly from 0.25 at lower T to 0.32 at the highest T and is similar to the value obtained by neutron backscattering techniques [28]. This means that in this temperature range we can assume that we are observing a direct crossover from the fast dynamical regime towards the α relaxation.

In the low temperature regime the lower β values found suggest the possibility of an intermediate dynamical regime just after the crossover time t_c and before the α relaxation regime. Our results suggest that in the case of PI-$d3$ only this possible intermediate regime is accessible in the time window of the IN6 instrument at the measured temperature range. However, our actual experimental accuracy does not allow us to obtain definite conclusions about this question. Concerning the fitting procedure, it is interesting to point out that we have considered τ_D and τ_{KWW} as free fitting parameters, i.e., we have not forced the above-mentioned Q dependence of these times. Moreover, in the case of the high temperature slow regime of PB we have used as the β parameter the average value for the three temperatures deduced from the $f(t)$ behavior, i.e., $\beta \cong 0.30$. Some representative fitting curves are shown in Fig. 5. These curves describe quite well the experimental $S(Q,t)$ behavior. By this fitting procedure we obtain the Q and T dependence of the characteristic times τ_D and τ_{KWW} corresponding to the fast and slow α relaxation regimes, respectively.

The behavior is shown in Fig. 6 for PB. Values of $\tau_{KWW}(Q)$ for the α relaxation of PB at 230 and 250 K, obtained from neutron backscattering measurements and taken from Ref. [28], have also been included for comparison. However, the values of $\tau_{KWW}(Q)$ from this reference and corresponding to 210 K were not considered because this temperature is lower than the temperature at which the α and β (slow) dielectric relaxations merge. Therefore it is not clear if the quasielastic behavior measured by IN13 only corresponds to the α process. At this point it is interesting to remark that the range of Q covered by the backscattering instrument used (IN13) was wider than that of the TOF (IN6) measurements. It turns out that the Q dependence found for τ_D and τ_{KWW}
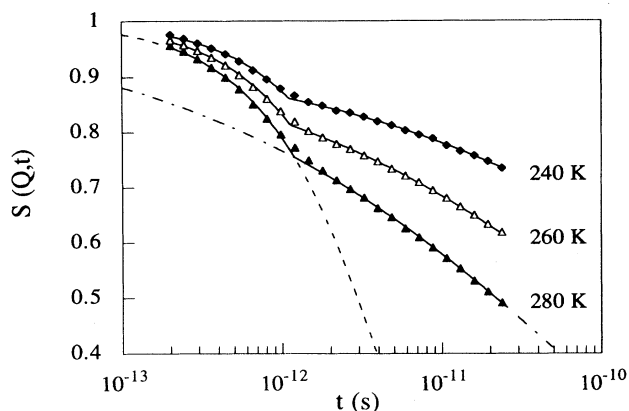
FIG. 5. $S(Q,t)$ for PB at $Q = 1.4$ Å^{-1} and different temperatures. Lines through the points are fitting curves according to expression (7) (see text).

is temperature independent within the experimental uncertainties. Moreover, the Q dependence of τ_{KWW} is the same for both the values of τ_{KWW} corresponding to TOF measurements and those from the backscattering measurements (IN13). It is interesting to point out that the latter were obtained not only from a different experimental technique but also by a more standard analysis procedure of the data directly performed in the frequency domain. Therefore the good agreement found between both sets of data gives additional support to the deconvolution procedure used in this work.

The results described above show that the temperature dependence and the Q dependence of both τ_D and τ_{KWW} can be factorized: $\tau(Q,T) = a(T)\tau(Q)$. Then, in both cases a master curve $\tau(Q)$, giving the Q dependence of
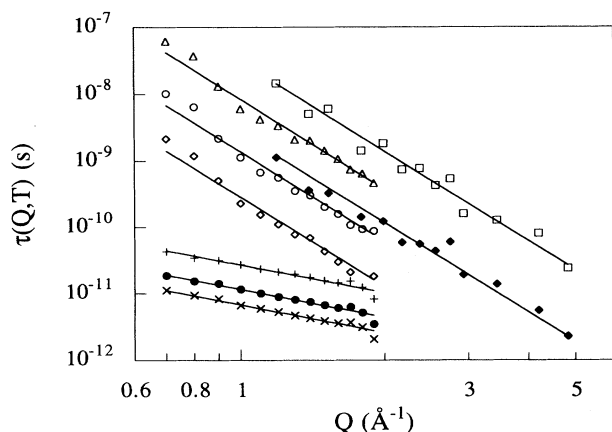
$\tau(Q,T)$, can be constructed by shifting the corresponding $\tau(Q,T)$ values in the logarithmic τ scale towards a reference value $\tau(Q,T_r)$. Here T_r is an arbitrary temperature of reference in the measured temperature range. Moreover, the shift factor values used for producing this master curve allow us to obtain the $a(T)$ behavior and therefore the temperature dependence of the $\tau(Q,T)$ considered. The master curves obtained for τ_D and τ_{KWW} in PB are shown in Fig. 7. The Q dependence found for a regression fit of these master curves is $\tau_D(Q) \propto Q^{-1.4}$ and $\tau_{KWW} \propto Q^{-4.5}$ (reference temperature 260 K).

From these functional forms and the expressions (5) and (7) we deduce a b value of $b \cong 1.4$ in good agreement with the b value found in the previous section (1.4) from the $f(t)$ construction [see Fig. 4(a)]. Similar results are obtained for τ_D in the case of PI-$d3$ giving $\tau_D(Q) \propto Q^{-1.3}$. Figure 8 shows the temperature dependence of τ_D and τ_{KWW} obtained for PB at $Q = 1.4$ Å^{-1}, yielding similar results to those from PVC reported in Ref. [10]. The values of τ_{KWW} obtained at 240, 260, and 280 K follow the same temperature dependence as the τ_{WW} obtained by backscattering techniques (analyzed in the frequency domain) at 250 and 230 K, as well as the temperature dependence of the viscosity time scale [28]. Therefore, as in the case of PVC [10], the results obtained by TOF confirm the results obtained for the α relaxation in a different time scale by backscattering techniques. Once again this gives additional support to our analysis procedure. The temperature dependence of τ_D follows an Arrhenius-like behavior, $\tau_D(T) = \tau_0\exp[E/k_B T]$, with an activation energy $E \cong 1.9$ kcal/mol and a value of the preexponential factor of 1.1×10^{-13} s for $Q = 1.4$ Å^{-1}. Similar Arrhenius laws for τ_D are found for PB-$d6$ and PI-$d3$. In the case of PB-$d6$ (coherent scattering) Fig. 8 shows the temperature dependence of τ_D for two different Q values, $Q = 1.4$ and 1.9 Å^{-1}, corresponding to the first maximum and the first minimum of the static structure factor $S(Q)$, respectively. In this case, the activation en-
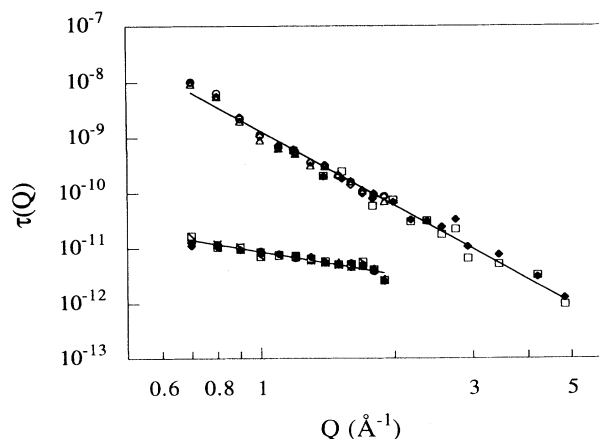

FIG. 6. Q dependence of the relaxation times τ_D and τ_{WW} for PB at different temperatures. τ_D: ($\times$) 280; ($\bullet$) 240; ($+$) 200 K. τ_{KWW}: ($\Diamond$) 280; ($\circ$) 280; ($\blacklozenge$) 250; ($\triangle$) 240; ($\square$) 230 K. The values of τ_{KWW} at 230 and 250 K are taken from Ref. [28] and correspond to backscattering measurements (see text). Lines through the points correspond to the law $Q^{-1.4}$ for τ_D and $Q^{-4.5}$ for τ_{KWW}.

FIG. 7. $\tau(Q)$ master plots obtained from data shown in Fig. 6 (see text) and giving the Q dependence of τ_D and τ_{KWW} for PB. Continuous lines through the points are linear regression fits (reference temperature 260 K).
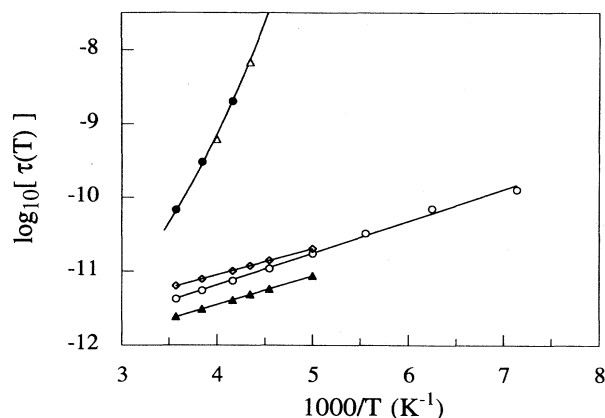
FIG. 8. Temperature dependence of the relaxation times τ_D and τ_{KWW} for PB. ($\bigcirc$) τ_D ($Q = 1.4$ Å^{-1}); ($\Diamond$) τ_D ($Q = 1.4$ Å^{-1}) corresponding to PB-$d6$; ($\blacktriangle$) τ_D ($Q = 1.9$ Å^{-1}) corresponding to PB-$d6$; ($\bullet$) τ_{KWW} ($Q = 1.4$ Å^{-1}) from TOF data; ($\triangle$) τ_{KWW} ($Q = 1.4$ Å^{-1}) from backscattering data. The continuous line through the τ_{KWW} data corresponds to the viscosity time scale.

ergy found, although about 2 kcal/mol too, is slightly dependent on Q. This point will be discussed below. The activation energy found for PI-$d3$ is around 2.7 kcal/mol. On the other hand, we have also compared the Q dependence of τ_D corresponding to both coherent and incoherent scattering. Figure 9 shows that in the Q range covered we can write $\tau_D^{coh} \propto \tau_D^{inc} S(Q)$, where the static structure factor $S(Q)$ has been calculated from the TOF (IN6) data. This behavior displays the so-called de Gennes narrowing [33], which can be established for quasielastic diffusionlike behavior. Therefore this result appears to give support to the physical idea behind the phenomenological analysis described above, i.e., the $S(Q,t)$ obtained through the deconvolution procedure used has a relaxational origin even in the short time regime. Moreover, the de Gennes−like relationship also explains the
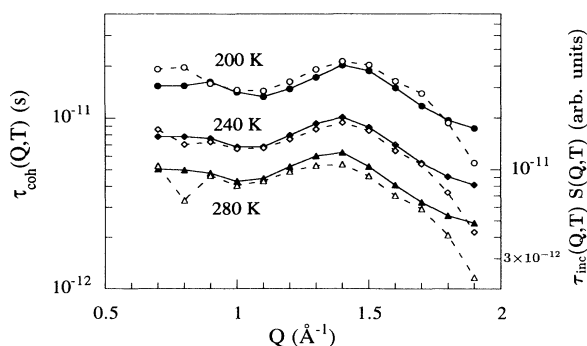

FIG. 9. Comparison between the τ_D values corresponding to coherent scattering (full symbols) and the τ_D values corresponding to incoherent scattering multiplied by the static structure factor $S(Q,T)$. Lines through the points are drawn to guide the eyes.

slight differences for the activation energy of τ_D^{coh} corresponding to the Q values of the first maximum and first minimum of $S(Q)$ respectively. These differences can be understood taking into account that $S(Q)$ of PB changes with temperature and that the change is stronger for the first maximum [31].

In the framework of the phenomenological analysis described above, the results can be interpreted as follows. First of all, it is worthy of remark that the expression used (7) for $S(Q,t)$ in fact implies that the two-step decay displayed by $S(Q,t)$ should correspond to only one dynamical process showing a complex relaxation function. The "shape" of this relaxation function $S(Q,t)$ depends on the time scale of observation and changes around the crossover time. If the process is observed through an instrument with a short time scale window ($t < t_c$), then the time dependence for $S(Q,t)$ can be approximately described by a single exponential decay. On the other hand, if the time window of the instrument is in the range $t > t_c$, then the time dependence can be quite well approximated by a KWW function, at least in the high temperature range (in the lower temperature range another functional form cannot be discarded as has been mentioned above). However, in both cases the preexponential factor of the exponential function or of the KWW function describing the normalized $S(Q,t)$ is close to 1.

Another interesting point is that the extent to which $S(Q,t)$ relaxes following the exponential or the KWW decay depends on both Q and temperature. At the high temperature limit, the whole of the decay would take place in the short time regime ($t < t_c$), and $S(Q,t)$ would approximately follow only an exponential decay. However, extrapolating our results, the temperature range at which this single exponential should be observed ($T \approx T_g + 300$ K for a $Q \cong 1$ Å^{-1}) is beyond the temperature range where a polymer is chemically stable. At the accessed Q and temperature range ($T \leq T_g + 100$ K, $Q \approx 1$ Å^{-1}) only a small fraction of $S(Q,t)$ decays following the exponential law (see, for example, Fig. 6). This implies that the deduced (by fitting) relaxation time τ_D ($\approx 10^{-11}$ s) is usually beyond the crossover time t_c.

If we identify the KWW behavior observed at $t > t_c$ (at least at high temperatures) with the α relaxation, then we have to associate the first exponential decay of $S(Q,t)$ with the short time regime of this α relaxation. Now we ask, what is the molecular origin of this short time regime, i.e., the molecular origin of the elementary motions involved in the α relaxation? Nowadays it is believed that in the case of glass-forming polymers the elementary motions involved in the α relaxation should be related to the conformational transitions which take place in the isolated chain [34]. However, the connection between the two dynamical processes is not clear up to now. The dynamics of conformational transitions in isolated chains is usually investigated by both experiments in very dilute solutions (NMR, etc.) and molecular dynamics (MD) simulations.

The activation energies found for conformational transitions are in the range of 2−5 kcal/mol [34], similar to the activation energies for the Debye regime found by us

from the temperature dependence of τ_D. In PB and PI-$d3$ (this work) we find E on the order of 2 kcal/mol. For PVC it was previously reported [10] that $E \approx 6$ kcal/mol, although a new careful analysis of the data, taking into account the improvements of the deconvolution procedure introduced here, gives a lower value $E \approx 4.5$ kcal/mol. It is interesting to point out that we obtain similar values of E for PB and PI-$d3$, i.e., for two polymers with similar chemical structure of the chain. This seems to indicate that the origin of the activation energy found is intramolecular, supporting the idea of identifying the exponential regime of $S(Q,t)$ with the conformational dynamics of the isolated chain, i.e., free from molecular interactions. One possible objection to this identification is that the relaxation function of the different theoretical models frequently used for describing the conformational dynamics of the chain (see, for example, the Hall-Helfand model [35]) is not a single exponential. However, it has been shown in a recent paper [36] that in the short time limit a single exponential decay of correlations is approached in all models. Moreover, a single exponential decay has recently been observed in the short time behavior of the first order torsion autocorrelation junction in cis-PB by molecular dynamics simulation when the contribution of the oscillatory motions is removed [37]. Therefore the exponential decay of $S(Q,t)$ in the short time regime ($t < t_c$) could be considered as an adequate approximation.

Finally, in the framework of the interpretation above, the meaning of the crossover time t_c should be the time at which the intermolecular correlations start to play a significant role concerning the segmental dynamics. Below t_c, the chain is not affected by its neighbors, and the conformational dynamics follows an approximate exponential behavior. After t_c, the short time behavior is modified towards a KWW-like relaxation function, at least in the high temperature range.

As was suggested by some of us in a previous paper [10] and mentioned in the Introduction, this interpretation recalls the basic ideas of the so-called coupling model proposed a long time ago by Ngai [11] for describing dynamical processes in complex correlated systems and in particular the suggested application of such a model to polymer dynamics [38].

B. The vibration relaxation model applied to PB and PI

A harmonic oscillator is characterized by a spring and the oscillating mass. The eigenfrequency is then given by the square root of the ratio of the two. If one goes to a molecule consisting of N atoms having the masses M_i ($i = 1, \ldots, N$) the vibrational properties are described by a dynamical matrix

$$D_{ij}^{\alpha\beta} = \frac{1}{\sqrt{M_i M_j}} \frac{\partial^2 V}{\partial u_{i\alpha} \partial u_{j\beta}} . \tag{8}$$

Here V is the interatomic potential, $u_{i\alpha}$ the displacement of atom i in direction α, and $D_{\alpha\beta}^{ij}$ the dynamical matrix. Such a matrix is symmetric and has n real eigenvalues λ_k ($k = 1, \ldots, 3N$) which are related to the eigenfrequencies

by $\omega_k^2 = \lambda_k$.

The eigenvectors describe the displacement pattern of the atoms

$$u_i = \sum_{k=1}^{3N} \frac{\mathbf{e}_{ik}}{\sqrt{M_i}} A_k , \tag{9}$$

where $\mathbf{e}_{ik}$ are the eigenvectors and A_k the normal coordinates. Finally, in terms of the normal coordinates the energy of the oscillating systems can be written as

$$E = \sum_{k=1}^{3N} [\tfrac{1}{2} \dot{A}_k^2 + \tfrac{1}{2}\lambda_k A_k^2 + O(A^3)] , \tag{10}$$

where the first term in the square brackets describes the kinetic and the second term the potential energy.

Compared to a molecule or a crystalline solid, the energy landscape in a glass is fundamentally different. As a consequence of the nonequilibrium glassy state, the potential surface can be understood as a multiminima structure. Therefore the local equilibrium positions of different atoms are not necessarily situated in the local energy minimum—it is even conceivable that an atom occupies a site at the top of an energy barrier—leading to eigenmodes with negative eigenvalues.

In such a frustrated multiminima energy landscape at least the part of the dynamic matrix dealing with low frequency excitations may be considered as a random symmetric matrix, where the different matrix elements are randomly distributed. Such random matrices were studied in the 1950s in connection with low lying excited states of complex nuclei. According to Wigner [22], the density distribution of eigenvalues of such a matrix forms a semicircle around the eigenvalue $\lambda = 0$. Thus positive and negative eigenvalues occur with the same probability.

This picture of a random matrix with a nearly constant density of eigenvalues around the origin is the starting point of our model, which tries to combine the low frequency excitations in glasses with the picture of low barrier relaxations [12]. This is performed in a single-mode picture where we can write down the Hamiltonian for each uncoupled normal coordinate separately:

$$H_\lambda = \tfrac{1}{2} \dot{A}_\lambda^2 + \frac{\lambda}{2} A_\lambda^2 + \frac{v_4}{4} A_\lambda^4 . \tag{11}$$

Here the nonharmonic fourth order term v_4 is needed in order to stabilize states with negative eigenvalues. Figure 10 displays typical potentials for a normal coordinate for positive and negative λ. For positive λ we mainly have harmonic vibrations, while for negative λ the fourth order term creates a double-well potential. In this potential vibrations both around the minimum positions as well as over the barrier relaxations are possible. From the potential energy part in Eq. (11) we can calculate the height of the barrier E_a,

$$E_a = \frac{\lambda^2}{4v_4} , \tag{12}$$

and the distance between the minimum positions $A_{\min}$,

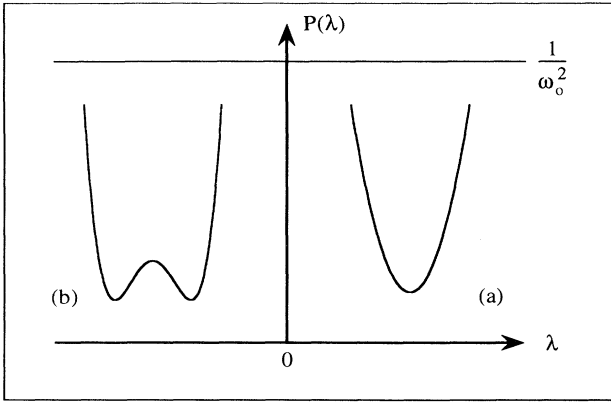$$A_{\min}^2 = \frac{|\lambda|}{v_4} . \tag{13}$$

FIG. 10. Typical potentials for a normal coordinate (a) positive eigenvalue and (b) negative eigenvalue.

From the second derivative of the potential function in the minima we get the vibrational frequencies $\omega_\lambda^2 = 2|\lambda|$. In order to describe the hopping rate Γ in between the two minima we use Kramers' result for over the barrier hopping in the weak coupling limit [23]:

$$\Gamma = \gamma \frac{E_a}{kT} e^{-E_a/k_B T} . \tag{14}$$

The weak coupling limit is a good approximation as long as the vibrational damping γ is small compared to the eigenfrequency ω_λ.

In order to come to a tractable model we now have to make a number of simplifying assumptions which are, summarized in the following.

(1) We assume a constant eigenvalue distribution $P(\lambda)$, implying a density of states proportional to ω, $g(\omega) = 3\omega/\omega_0^2$, where ω_0 is the first parameter of the model.

(2) The stabilizing fourth order term v_4 in Eq. (11) is assumed to be the same for all eigenmodes.

(3) The double-well potentials do not exhibit an asymmetry ($v_3 = 0$).

(4) The vibrations are treated classically using the

Langevin equation for the damped oscillator (see the Appendix). Thereby, for all vibrations we assume the same friction $\gamma = $const; γ is the second parameter of the model.

(5) For the density of states we use an empirical formula which approaches the correct low and high frequency limits

$$g(\omega) = \frac{3\omega^2}{\omega_0^2} \left[\frac{a + \omega^2}{b + \omega^4} \right]^{1/2} ,$$

$$a = \frac{\omega_0^4 \omega_b^4}{\omega_D^6 - 2\omega_0^4 \omega_b^2} , \quad b = \frac{\omega_D^6 \omega_b^4}{\omega_D^6 - 2\omega_0^4 \omega_b^2} . \tag{15}$$

For small ω $g(\omega)$ approaches the sound wave limit $3\omega^2/\omega_D^3$. For large ω Eq. (15) yields the density of states of the random matrix. In between, $g(\omega)/\omega^2$ exhibits a maximum—the boson peak. The third parameter of the model is the boson frequency ω_b. The Debye frequency ω_D can be taken from high frequency sound wave experiments like Brillouin scattering. In the actual fits it was the fourth varied parameter.

(6) In order to relate the mean squared displacements, which are the measured quantities, to the normal coordinates an equipartition of amplitudes according to Eq. (16) is assumed:

$$\sum_{i=1}^{N} \langle x_{ik}^2 \rangle = \sum_{i=1}^{N} \frac{e_{ik}^2}{M_i} \langle A_k^2 \rangle \approx \frac{\langle A_k^2 \rangle}{\overline{M}} . \tag{16}$$

Equation (16) describes the contribution of one normal coordinate A_k to the average atomic displacement. The sum here is taken over all atoms of the glass.

(7) For the hopping motion across the well of the double-minimum potential Kramers' weak damping case is assumed [see Eq. (14)].

(8) Finally, the relaxations will be treated in Gaussian approximation.

On the basis of this greatly simplified model now the dynamic structure factor $S(Q,t)$ will be calculated. Equation (A8) of the Appendix gives the incoherent intermediate scattering function for a single damped oscillator [39]. Inserting the density of states Eq. (15) the incoherent scattering function of the vibrating ensemble becomes

$$S(Q,t)_{\text{vib}} = \exp \left[-\frac{Q^2 k_B T}{M} \left\{ \int_0^{\omega_c} \frac{g(\omega)}{\omega^2} \left[1 - e^{-(\gamma/2)t} \left[\frac{\gamma}{2\tilde{\omega}} \sin\tilde{\omega}t + \cos\tilde{\omega}t \right] \right] d\omega \right\} \right] . \tag{17}$$

Here, ω_c is the cutoff frequency which follows from the normalization requirement. This is approximately fulfilled for $\omega_c^2 = 2\omega_0^2/3$. The frequency of the damped oscillator $\tilde{\omega} = \sqrt{\omega^2 - \gamma^2/4}$ may become imaginary without invalidating the result.

The consideration of incoherent scattering from vibrations in the time domain has the invaluable advantage

that there the scattering function can be calculated analytically without resorting to any order of phonon approximation. In other words, $S(Q,t)$ in Eq. (17) includes all multiphonon contributions.

For the relaxational part we have to consider hopping motion in a double-well potential. Assuming for simplicity double wells of equal depth with a jump distance d_λ

and a jump rate Γ_λ, the orientationally averaged intermediate incoherent scattering function has the form

$$S(Q,t)_{\mathrm{rel}} = \tfrac{1}{2}\{[1+j_0(Qd_\lambda)]+[1-j_0(Qd_\lambda)]e^{-2t\Gamma_\lambda}\} \quad (18)$$

with $j_0(x)$ denoting the spherical Bessel function of zero order. The first part of Eq. (18) is the elastic incoherent structure factor (EISF); the second part contains the information on the time scale of motion. For small jump distances we expand $j_0(x) \approx 1 - x^2/6$ and obtain

$$S(Q,t)_\lambda = 1 - \frac{(Qd_\lambda)^2}{12}(1-e^{-2t\Gamma_\lambda}) . \quad (19)$$

In the next step we have to average over the distribution $P(\lambda)$. For this we consider only those double wells where the barrier is larger than $k_B T$. With the barrier height $E_a = \lambda^2/4v_4$ [Eq. (12)] and using the relation between normal coordinates and mean square displacement [Eq. (16)], Eq. (13) yields for the jump distance $d_\lambda^2 = 4|\lambda|/(Mv_4)$. With the jump rate

$$\Gamma_\lambda = \gamma \left[\frac{\lambda^2}{4v_4 k_B T} \right] e^{-\lambda^2/4v_4 k_B T}$$

[Eq. (14)] we have

$$S(Q,t)_{\mathrm{rel}} = 1 - \frac{2}{3}\frac{k_B T}{M}Q^2 \int_{\sqrt{4k_B Tv_4}}^{\infty} P(\lambda)\frac{\lambda\,d\lambda}{2v_4 k_B T}(1-e^{-2t\gamma(\lambda^2/4v_4 k_B T)e^{-\lambda^2/4v_4 k_B T}}) . \quad (20)$$

Substituting $\lambda^2/(4v_4 k_B T)=\xi$ and inserting $P(\lambda)=3/\omega_0^2$ Eq. (20) transforms to

$$S(Q,t)_{\mathrm{rel}} = 1 - \frac{2Q^2 k_B T}{M\omega_0^2} \int_1^\infty d\xi(1-e^{-2t\gamma\xi e^{-\xi}}) . \quad (21)$$

Finally, exponentiating Eq. (21), the relaxational incoherent intermediate scattering function becomes

$$S(Q,t)_{\mathrm{rel}} \cong \exp\left\{ -\frac{2Q^2 k_B T}{M\omega_0^2} \int_1^\infty d\xi(1-e^{-2t\gamma\xi e^{-\xi}}) \right\} . \quad (22)$$

The total scattering function $S(Q,t)$ is then obtained as the product of $S(Q,t)_{\mathrm{vib}}$ and $S(Q,t)_{\mathrm{rel}}$, which may also be written as

$$S(Q,t)=\exp\left\{ -\frac{Q^2}{3}[u_{\mathrm{vib}}^2(t)+u_{\mathrm{rel}}^2(t)] \right\} . \quad (23)$$

Equation (23) constitutes the final result for the incoherent scattering function of the vibration relaxation model.

The data evaluation presented in Sec. III was based on the assumption that the scattering from the low frequency phonons properly Bose scaled to higher temperature could be subtracted from the actual spectra in order to obtain the relaxational contributions. In the framework of the presented vibrational relaxation model this treatment of the low temperature phonons is not adequate in principle. However, in order to be able to compare with the presented data we subtract the Bose-scaled contribution of the low temperature phonons also in our theoretical function, which then yields

$$S(Q,t)=\exp\left\{ -\frac{Q^2}{3}\{u_{\mathrm{vib}}^2(t)-[u_{\mathrm{vib}}^{\mathrm{harm}}(t)]^2+u_{\mathrm{rel}}^2(t)\} \right\} , \quad (24a)$$

$$(u_{\mathrm{vib}}^{\mathrm{harm}})^2 = \frac{k_B T}{M} \int_0^{\omega_{\mathrm{harm}}} \frac{g_{\mathrm{harm}}(\omega)}{\omega^2}(1-\cos\omega t)d\omega . \quad (24b)$$

The parameters for the harmonic density of states for PB are obtained from a fit to the spectrum at 100 K. The application of the phenomenological equation for the density of states [Eq. (15)] needs as an input the Debye frequency resulting from the sound waves,

$$\frac{3}{\omega_D^3} = \frac{V_a}{6\pi^2} \left[\frac{1}{v_l^3} + \frac{2}{v_t^3} \right] , \quad (25)$$

where v_l and v_t are the longitudinal and transverse sound velocities, respectively, and V_a is the monomeric volume. The Debye frequency ω_D is taken as a fit parameter and later compared to an "experimental value" estimated from Brillouin sound velocities.

Including the harmonic mean square displacement $(u_{\mathrm{vib}}^{\mathrm{harm}})^2$ [Eq. (24b)] we fitted Eq. (24a) to the Fourier transformed deconvoluted spectra (see Sec. IV), varying the constant eigenvalue density $3/\omega_0^2$, the boson peak frequency ω_b, the phonon damping rate γ, and the Debye frequency ω_D. Figure 11 compares the deconvoluted PB spectra taken at $Q=1.4$ Å^{-1} with the calculated curves at seven different temperatures.

As can be seen from the comparison of the theoretical and experimental scattering functions the agreement between model and experiment is excellent at times shorter than about 10 ps. The most salient feature of the data, namely, the two-step character of the decay process in $S(Q,t)$, is depicted very well by the model. This is also true for the detailed shape of the scattering function. The first decay at times shorter than about 2 ps mainly results from the low frequency vibrations, which in this model are shifted with increasing temperature towards lower frequencies. The second part—the long time tail—originates from the relaxational part of the scattering function and is due to the jump motion across the
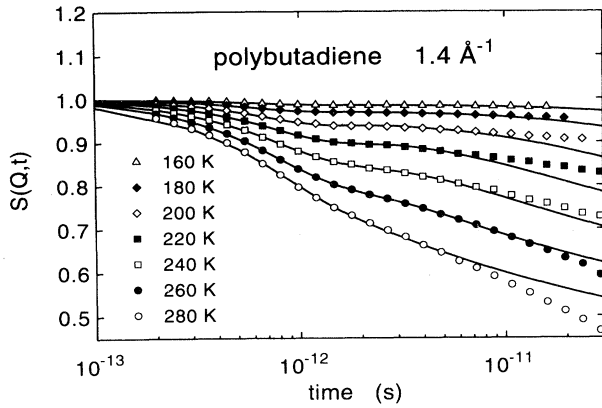
FIG. 11. Fits of the polybutadiene data of Fig. 3(a) with the vibration relaxation model.

FIG. 12. Fits to polybutadiene data in ω space with the vibration relaxation model. The arrows indicate the contribution of the sound waves to the density of states at the respective temperatures. Thereby the level increases with temperature.

double-well potentials. In this relaxational regime for long times the model at low temperatures overestimates and at higher T underestimates the experimental decay of the scattering function. The too strong decay of the theoretical model at low T can be understood because all assumptions concerning the hopping motion in the double-well potential tend to overestimate the corresponding rates. (i) Kramers' weak coupling limit gives the maximum possible relaxation rate. (ii) The neglect of asymmetry in the potential gives rise to a too strong contribution of fast hopping processes. At higher temperatures additional relaxation processes occur which are not depicted by the vibration relaxation model. It is straightforward to reason that those extra relaxations are most likely due to the onset of the α relaxation. Its short time part appears to move into the observation window. Naturally, the vibration relaxation model cannot describe these structural relaxations, which give rise to the flow processes.

In order to scrutinize the consistency of the Fourier transformation and deconvolution procedures we also fitted the dynamic structure factor $S(Q,\omega)$ resulting from our model directly to data in ω space. For this purpose we used the one-phonon approximation and excluded the elastic part. The theoretical scattering function, thereby, was convoluted with the spectrometer resolution function. Figure 12 displays such a fit to time-of-flight data taken on IN6 with neutrons of 4.1 Å wavelength. For the three temperatures shown again an excellent fit is obtained.

Figures 13 and 14 present the resulting model parameters as a function of temperature. There, the circles represent the parameters from the fit in ω space while the squares denote the outcome of the fit in the time domain. As can be seen, a consistent set of parameters evolves.

The most prominent outcome is the pronounced softening of the boson peak frequency ω_b which sets in already well below the glass transition temperature ($T_g = 186$ K) and leads to its extinction around room temperature. Such a strong downward shift of the Boson peak cannot easily be explained via a Grüneisen relation
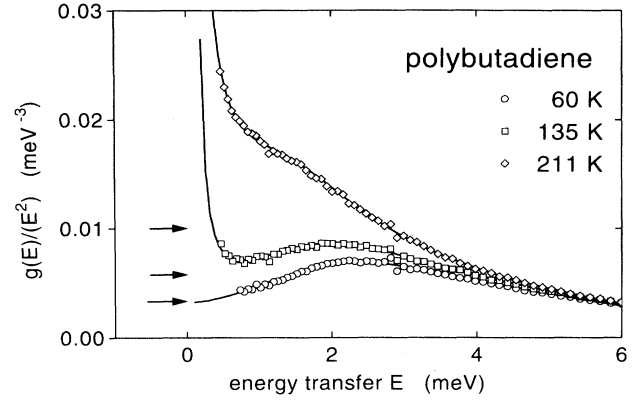
working on the basis of thermal expansion. Taking the literature values [40] for the thermal (volume) expansion $\alpha_g = 1.8 \times 10^{-4}$ K^{-1} in the glass phase and $\alpha_l = 6 \times 10^{-4}$ K^{-1} in the liquid phase, the strong softening of the boson peak requires a mode Grüneisen $\gamma_i = \partial\ln\omega_i / \partial\ln V$ of 15.5 in both phases. If one calculates a thermal Grüneisen parameter $\gamma_T = \alpha B / \rho C_v$ at 100 K, taking measured specific heat data [41], the bulk modulus B from the sound velocities [42], and the density $\rho = 890$ kg/m^3, one obtains $\gamma_T = 2.8$. So the boson peak would have to be six times more sensitive to volume changes than the average vibrational mode. On the other hand, the longitudinal sound waves have a mode Grüneisen γ of 5.5, also considerably more than the average. The clarification of this question remains a challenging task for the future.
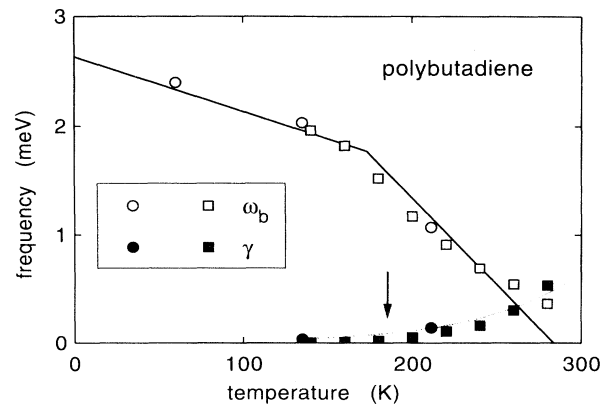

FIG. 13. The model parameters ω_b (boson peak frequency) and γ (vibrational friction) resulting from the vibration relaxation model fits of polybutadiene as a function of temperature. The solid line corresponds to the mode Grüneisen parameter discussed in the text. The dotted line displays $\langle u^2 \rangle^2 / T$ [see Eq. (27)].
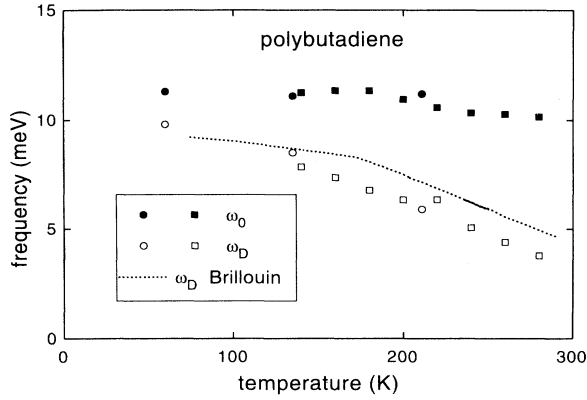
FIG. 14. The model parameters ω_0 (normalization frequency) and ω_D (Debye frequency) of the vibration relaxation model fits of polybutadiene as a function of temperature.

FIG. 15. Sound velocities in polybutadiene as a function of temperature (see text [42]).

According to Eq. (A2) the phonon damping γ is proportional to the average square of the stochastic force divided by the temperature. Considering third order interaction as a main cause for anharmonicity the stochastic force f_k, acting on mode k, results from the third order term in the potential,

$$f_k \approx \sum_{l,m} V_3 A_l A_m \ , \tag{26}$$

or, following Eq. (16), the stochastic force squared is proportional to the square of the mean squared displacement $\langle u^2 \rangle^2$. With this relation the phonon damping $\gamma(T)$ can be written as

$$\gamma(T) \approx \frac{\langle u^2 \rangle^2}{T} \ . \tag{27}$$

Using the vibrational mean square displacements obtained from the data evaluation in terms of Eq. (23) we have calculated the prediction of Eq. (27). The solid line in Fig. 13 compares the calculation with the experimental values. A good agreement between the results of the vibrational relaxation model and the estimation of phonon damping due to third order interactions can be obtained.

Figure 14 displays the two parameters determining the density of states. While ω_0, the parameter responsible for the density of states due to the random matrix, is basically temperature independent, the Debye frequency ω_D due to the sound waves drops by about a factor of 2. Figure 15 presents Brillouin scattering results by Krüger [42] for the longitudinal sound velocity v_l as a function of temperature. The figure also includes a low temperature result for the transverse velocity v_t. The temperature dependence is characterized by a weak softening of the sound velocity below T_g and a strong drop above this temperature. Using an empirical relation between v_t and v_l which holds, e.g., for polycarbonate of 2,2-bis(4-hydroxyphenyl)-propane (BPA-PC) [20],

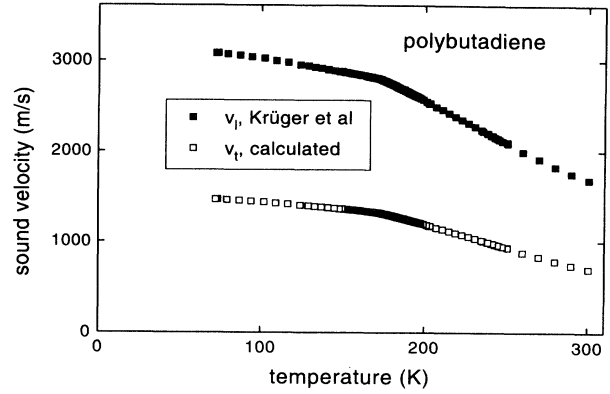$$\frac{v_{t0}^2 - v_t^2}{v_{l0}^2 - v_l^2} = \frac{1}{4} \ , \tag{28}$$

where v_{t0} and v_{l0} are reference sound velocities at low temperature, v_t was estimated and included in Fig. 15. With these sound velocities and the temperature dependent density of PB the Debye frequency ω_D was calculated according to Eq. (25). The result is shown as a dotted line in Fig. 14. Apart from an upward shift of about 1 meV the fitted Debye frequencies and the Brillouin data agree well over the investigated temperature range, showing again the consistency of the approach.

As can be seen from Fig. 14, in the investigated temperature range the Debye frequency due to sound waves changes by about 50%. Consequently, the sound wave density of states, which changes with the third power of the Debye frequency, increases by a factor of 8. In order to judge the contribution of the sound waves to the total density of states the low temperature result for $g(\omega)/\omega^2$ displayed in Fig. 12 may serve as a guide. There, the contribution of sound waves to the spectrum can be read off as the $E \rightarrow 0$ limit, being a very substantial part of the total spectrum. On increasing the temperature to 280 K, this contribution is expected to increase by a factor of about 8. Thus approximating the temperature dependence of the vibrational contribution to the spectrum by a temperature extrapolation of the harmonic, low temperature density of states underestimates at least significantly the changes of the sound wave density of states. On the other hand, the nearly constant density of states for the random matrix modes reflects the experimental fact of a seemingly harmonic temperature dependence of the spectra at higher frequencies, which is found rather generally in glasses.

VI. CONCLUSIONS

The first result of this paper is to corroborate the finding of two different time regimes in the dynamics of polymers at the glass transition temperature range and above. This implies that the behavior previously found in PVC [10] appears to be a general feature of glass-forming polymers (and probably of glass-forming systems in general) and it is not a consequence of the particular charac-

ter of PVC.

The crossover time t_c separating the two dynamical regimes is of the order of 2 ps and seems to depend neither on temperature nor on Q. This makes it difficult to interpret this process as the β process of the mode coupling theory, as has usually been done in the recent literature [6–8]. As far as PB is concerned, that difficulty was already noted in earlier mode coupling fits of the susceptibility behavior obtained from TOF data [28]. These fits failed to show the expected shift of the susceptibility minimum with temperature and the scaling behavior.

In this paper we have shown that the fast process could be satisfactorily described by two different models. In the first [10], once the harmonic phonons are removed, the fast process emerges as a Debye regime of the slower relaxation process (α relaxation). This fast regime can be associated with the conformational transitions in the macromolecular chain free from intermolecular interactions. In this framework t_c means the time at which these interactions start to play a significant role in the dynamics. In the second model, the fast process has a vibrational origin and it is ascribed to the softening of the vibrational boson peak with increasing temperature. In this framework, t_c means the crossover time between vibrations and relaxations. Since both models give a good fit to the available data, neutrons are obviously unable, up to date, to decide whether one deals with fast relaxations or vibrational softening. However, the results have important implications in either one of the two cases. In the vibrational softening case, the results imply an exceedingly high mode Grüneisen parameter of the modes at the boson peak, considerably higher than that of the Brillouin sound waves. It is difficult to conceive an explanation for such a strong anharmonicity. On the other hand, the Brillouin phonons do indeed show a considerable softening with increasing temperature. This fact has to be taken into account in future versions of the relaxation model in order to improve the harmonic approximation used to remove the phonon component from the scattering spectra.

ACKNOWLEDGMENTS

APPENDIX: SCATTERING CROSS SECTION FOR A DAMPED HARMONIC OSCILLATOR

In the following we calculate the incoherent intermediate dynamic scattering function $S(Q,t)$ for a damped harmonic oscillator in the classical approximation. The Langevin equation for a damped oscillator reads

$$\frac{d^2}{dt^2}x + \gamma\frac{d}{dt}x + \omega_0^2 x = f(t) , \qquad (A1)$$

where x is a generalized coordinate, ω_0 the eigenfrequency, γ the damping, and $f(t)$ the random force. For the random forces we assume white noise, resulting in

$$\langle f(t)f(t')\rangle = \frac{2k_B T}{m}\gamma\delta(t-t') . \qquad (A2)$$

Here, m is the oscillating mass and T the temperature. k_B denotes the Boltzmann constant and the angular brackets indicate a thermal average. Using the oscillator Green function

$$G(t) = \frac{\Theta(t)}{\tilde{\omega}}e^{-(\gamma/2)t}\sin\tilde{\omega}t , \qquad (A3)$$

where $\Theta(t)$ is the step function and $\tilde{\omega}^2 = \omega_0^2 - \gamma^2/4$, Eq. (A1) is solved as

$$x(t) = \frac{1}{\tilde{\omega}}\int_{-\infty}^t A(\xi)e^{-(\gamma/2)(t-\xi)}\sin[\tilde{\omega}(t-\xi)]d\xi . \qquad (A4)$$

In order to calculate the scattering function we need the correlation function

$$\langle x(t)x(0)\rangle = \frac{1}{\tilde{\omega}^2}\int_{-\infty}^t\int_{-\infty}^0 \langle A(\xi)A(\eta)\rangle e^{-(\gamma/2)(t-\xi-\eta)}$$
$$\times\sin[\tilde{\omega}(t-\xi)]$$
$$\times\sin[\tilde{\omega}(-\eta)]d\xi\,d\eta . \qquad (A5)$$

With Eq. (A2) the correlator becomes

$$\langle x(t)x(0)\rangle = \frac{k_B T}{m\omega_0^2}e^{-(\gamma/2)t}\left\{\frac{\gamma}{2\tilde{\omega}}\sin\tilde{\omega}t + \cos\tilde{\omega}t\right\} . \qquad (A6)$$

In Gaussian approximation, which is exact for harmonic oscillators, the intermediate scattering function reads

$$S(Q,t)_{\text{vib}} = \exp\left\{-\frac{Q^2}{3}\{\langle[x(0)]^2\rangle - \langle x(t)x(0)\rangle\}\right\} . \qquad (A7)$$

With the result of Eq. (A6) we finally get

$$S(Q,t)_{\text{vib}} = \exp\left\{-\frac{Q^2 k_B T}{3M\omega_0^2}\right.$$
$$\left.\times\left[1 - e^{(\gamma/2)t}\left[\frac{\gamma}{2\tilde{\omega}}\sin\tilde{\omega}t + \cos\tilde{\omega}t\right]\right]\right\} . \qquad (A8)$$

This solution is also valid for imaginary $\tilde{\omega}$, transforming the trigonometric to hyperbolic functions. In order to relate to quantum mechanics we consider the appropriate quantum mechanical expressions for the harmonic oscillator correlation function:

$$\langle[x(0)]^2\rangle = \frac{\hbar}{2M\omega_0}(2\langle\hat{a}^\dagger\hat{a}\rangle + 1)$$
$$= \frac{\hbar}{2M\omega_0}\left[\frac{2}{e^{\hbar\omega_0/k_B T}+1} + 1\right] \approx \frac{k_B T}{M\omega_0^2} , \qquad (A9)$$

where $\hat{a}^\dagger$ and $\hat{a}$ are the phonon creation and annihilation

operators. The $\approx$ sign is valid for high temperatures. Correspondingly, for the high temperature expression of the distinct time correlator we have

$$\langle x(t)x(0)\rangle = \frac{k_B T}{M\omega_0^2}\cos\omega t \ . \tag{A10}$$

Thus the quantum mechanical high temperature approxi-

mation of $S(Q,t)$ becomes, in analogy to Eq. (A7),

$$S(Q,t)=\exp\left\{-\frac{Q^2 k_B T}{3M\omega_0^2}(1-\cos\omega_0 t)\right\} \ . \tag{A11}$$

Equation (A11) corresponds to the undamped classical scattering function.

[1] F. Fujara and W. Petry, Europhys. Lett. **4**, 921 (1987).

[2] B. Frick, D. Richter, W. Petry, and U. Buchenau, Z. Phys. B **70**, 73 (1987).

[3] C. H. Wang and R. B. Wright, J. Chem. Phys. **55**, 3300 (1970).

[4] R. Shuker and R. W. Gammon, Phys. Rev. Lett. **25**, 222 (1970).

[5] W. Götze, in *Liquids, Freezing and the Glass Transition*, edited by J. P. Hansen, D. Levesque, and J. Zinn-Justin (North-Holland, Amsterdam, 1991), p. 287.

[6] W. Knaak, F. Mezei, and B. Farago, Europhys. Lett. **7**, 529 (1988).

[7] B. Frick, B. Farago, and D. Richter, Phys. Rev. Lett. **64**, 2921 (1990).

[8] J. Wuttke, M. Kiebel, J. Bartsch, F. Fujara, W. Petry, and H. Sillescu, Z. Phys. B **91**, 357 (1993).

[9] U. Buchenau, M. Monkenbusch, M. Stamm, C. F. Majkrzak, and N. Nücker, in *Polymer Motion in Dense Systems*, edited by D. Richter and T. Springer, Springer Proceedings in Physics Vol. 29 (Springer, Berlin, 1988), p. 138.

[10] J. Colmenero, A. Arbe, and A. Alegría, Phys. Rev. Lett. **71**, 2603 (1993).

[11] K. L. Ngai and Y. F. Yee, J. Polym. Sci. Part B **29**, 1493 (1991).

[12] U. Buchenau, C. Schönfeld, D. Richter, T. Kanaya, K. Kaji, and R. Wehrmann, Phys. Rev. Lett. **73**, 2344 (1994).

[13] J. Colmenero, J. Non-Cryst. Solids **131-133**, 860 (1991).

[14] K. L. Ngai, A. Arbe, and J. Colmenero, in *Quasielastic Neutron Scattering*, Proceedings of the Conference on Quasielastic Neutron Scattering, San Sebastian, Spain, 1993, edited by J. Colmenero, A. Alegría, and J. Bermejo (World Scientific, Singapore, 1994), p. 277.

[15] K. L. Ngai, Comments Solid State Phys. **9**, 128 (1979); for an updated review, see K. L. Ngai, in *Disordered Effects in Relaxation Processes*, edited by R. Richert and A. Blumen (Springer-Verlag, Berlin, 1994).

[16] The fragility D is defined by Angell [see, for example, C. A. Angell, J. Non-Cryst. Solids **131-133**, 13 (1991)] as an exponent in the Vogel-Fulcher expression for the viscosity $\eta=\eta_0\exp[DT_0/(T-T_0)]$, where T_0 represents the Vogel temperature. A glass former is called fragile if the viscosity diverges rapidly as T varies from T_0 in contrast to strong systems, which show simple activation behavior.

[17] A. P. Sokolov, E. Rössler, A. Kisliuk, and D. Quitmann, Phys. Rev. Lett. **71**, 2062 (1993).

[18] F. Viras and T. A. King, J. Non-Cryst. Solids **119**, 65 (1990).

[19] B. Frick and D. Richter, Phys. Rev. B **47**, 14 795 (1993).

[20] G. D. Patterson, J. Polym. Sci. Polym. Phys. Ed. **14**, 741 (1976).

[21] L. Börjesson, A. K. Hassan, L. M. Torell, and A. Fontana, Phys. Rev. Lett. **70**, 1275 (1993).

[22] E. P. Wigner, Ann. Math. **67**, 325 (1958).

[23] H. A. Kramers, Physica (Utrecht) **7**, 284 (1940).

[24] M. Morton and L. J. Fetters, Rubber Rev. **48**, 359 (1975).

[25] J. T. Gotro and W. W. Graessley, Macromolecules **17**, 2767 (1984).

[26] D. Boese and F. Kremer, Macromolecules **23**, 829 (1990).

[27] B. Frick, Prog. Colloid Polym. Sci. **80**, 164 (1989).

[28] R. Zorn, D. Richter, B. Frick, and B. Farago, Physica A **201**, 52 (1993).

[29] It has to be conceded that the Bose–Debye-Waller scaling property is fulfilled as well for PI-*d*3 as for PB and PB-*d*6. The reason for this may be residual scattering from the methyl group.

[30] J. Colmenero, A. Alegría, J. M. Alberdi, F. Alvarez, and B. Frick, Phys. Rev. B **44**, 7321 (1991); F. Alvarez, A. Alegría, and J. Colmenero, *ibid.* **44**, 7306 (1991).

[31] B. Frick, D. Richter, and C. L. Ritter, Europhys. Lett. **9**, 557 (1989).

[32] J. Colmenero, Physica A **201**, 38 (1993); J. Colmenero, A. Arbe, A. Alegría, and K. L. Ngai, J. Non-Cryst. Solids **172-174**, 229 (1994).

[33] P. G. de Gennes, Physica **25**, 825 (1959).

[34] See as representative papers R. Dejean de la Batie, F. Laupetre, and L. Monnerie, Macromolecules **22**, 122 (1989); David B. Adolf and M. D. Ediguer, *ibid.* **24**, 5834 (1991); T. Radiotis, G. R. Brown, and Photis Dais, *ibid.* **26**, 1445 (1993); Richard H. Boyd, Richard H. Gee, Jie Hand, and Yong Jin, J. Chem. Phys. **101**, 788 (1994); Richard H. Gee and Richard H. Boyd, *ibid.* **101**, 8028 (1994).

[35] C. K. Hall and E. J. Helfand, J. Chem. Phys. **77**, 3275 (1982).

[36] Ivet Bahar, Burak Erman, G. Fytas, and W. Steffen, Macromolecules **27**, 5200 (1994).

[37] Eung-Gun Kim and Wayne L. Mattice, J. Chem. Phys. **101**, 6242 (1994).

[38] K. L. Ngai and R. W. Rendell, J. Non–Cryst. Solids **131-133**, 942 (1991).

[39] G. E. Uhlenbeck and L. S. Ornstein, Phys. Rev. **36**, 823 (1930).

[40] D. W. van Krevelen, *Properties of Polymers* (Elsevier, Amsterdam, 1976), p. 71.

[41] J. Grebowicz, W. Aycock, and B. Wunderlich, Polymer **27**, 575 (1986).

[42] Longitudinal sound velocity between 60 and 300 K: J. R. Krüger (private communication). The transverse ones were calculated as indicated in the text, using as a starting point the ultrasonic sound velocity at 77 K from A. Bhattacharya, T. L. Smith, and A. C. Anderson, J. Noncryst. Solids **31**, 395 (1979).